The Effects of Chemical Structure and Synthesis Method on Photodegradation of Polypropylene

Longxiang Tang, Qianghua Wu, Baojun Qu

State Key Laboratory of Fire Science and Department of Polymer Science and Engineering, University of Science and Technology of China, Hefei, Anhui 230026, People's Republic of China

Received 27 January 2004; accepted 16 June 2004
DOI 10.1002/app.21272
Published online in Wiley InterScience (www.interscience.wiley.com).

ABSTRACT: The effects of chemical structure and synthesis method on the photodegradation behavior of polypropylene (PP) were investigated in injection-molded samples exposed to ultraviolet radiation (UV) at 60°C. For this purpose, three PP samples with different chemical structures were chosen: two homopolymerized PP samples (H_1P, synthesized by bulk polymerization; whereas H_2P was synthesized by Ziegler–Natta catalyst) and copolymerized PP sample (CP). The photodegradation was characterized by melt flow rate and mechanical properties and Fourier transform infrared spectroscopy, X-ray photoelectron spectroscopy, and scanning electron microscopy. The results showed that CP possesses the most superior resistance to UV-irradiation, followed by H_2P and then H_1P, which indicates that copolymerization with a small amount of ethylene monomer is an effective approach to obtain high stability of PP to UV-irradiation, and synthesis methods of PP play an important role in the resistance to UV-irradiation. Moreover, the effect of photodegradation on the thermal behaviors of H_2P was also investigated using X-ray diffraction, differential scanning calorimetry, and dynamical mechanical thermal analysis. © 2004 Wiley Periodicals, Inc. J Appl Polym Sci 95: 270–279, 2005

Key words: photodegradation; chemical structure; homopolymerized polypropylene; copolymerized polypropylene; thermal behavior

1. INTRODUCTION

It has been recognized that stabilization against different modes of degradation is necessary if the use-life of a polymer is to be extended sufficiently to meet design requirements for long-term applications, especially for outdoor use. Almost all polyolefins are subjected to ultraviolet (UV)-induced degradation. In particular, polypropylene (PP) is prone to be photodegraded due to its structural characteristic, resulting in the deterioration of mechanical properties. In recent years, attention has been attracted to the oxidation of PP initiated photochemically, thermally, and radiochemically, and the mechanism by which oxidation occurs can be considered fairly well understood.[1] Nishimoto and colleagues investigated the effect of morphology of PP on its degradation due to γ-ray irradiation.[2,3] Rabello and White investigated the role of physical structure and morphology in the photodegradation behavior of PP[4,5] and found that the initial physical structures of PP, which include the degree of crystallinity, crystal, and molecular orientation, as well as crystal size, influence the photooxidation by affecting the oxygen permeability and UV absorption characteristics. Zhang et al. studied the wavelength sensitivity of photooxidation of PP.[6] Qiao and colleagues investigated the effect of isotacticity on the γ-irradiation resistance of PP.[7,8] Yishii et al. found that copolypropylene with 6% ethylene has better γ-irradiation stability, and different irradiation methods exert different influence on the oxidation behavior of PP.[9] However, few studies have been carried out on the effect of chemical structure, such as repeat unit and synthesis methods of PP, on the UV-induced degradation of PP. The aim of this paper is to discuss the effects of repeat unit and synthesis methods of PP on its photodegradation under high-intensity UV irradiation and the consequent changes in the mechanical and thermal properties.

Correspondence to: B. Qu (qubj@ustc.edu.cn).
Contract grant sponsor: National Natural Science Foundation of China; contract grant number: 50073022; contract grant sponsor: China NKBRSF Project; contract grant number: 2001CB409600.

EXPERIMENTAL

Materials

H_1P is a homopolypropylene synthesized by bulk polymerization with a wider molecular weight distribution. H_2P is also a homopolypropylene synthesized by Ziegler–Natta catalyst. Both were supplied by Yangzi

TABLE I
Characteristic Parameters of Different PP Samples

Sample code	Ethylene content (mol %)	Melt flow rate (g/10 min)	Crystallinity[a] (%)	Isotacticity[b] (%)
H_1P	—	6.0	27.4	95.62
H_2P	—	2.8	31.2	95.37
CP	5	1.3	15.4	90.17

[a] Obtained from the DSC runs at 20°C/min from 60 to 200°C in a Perkin–Elmer DSC-2.
[b] Obtained from the IR ratio of Abs. (997 cm^{-1})/Abs. (973 cm^{-1}).

Petrochemical Co. Ltd. (China). Copolypropylene (CP) with an ethylene content of 5% was supplied by Yanshang Petrochemical Co. Ltd. (China). The main characteristic parameters of three kinds of PP used in the present work are summarized in Table I.

Sample preparation

The samples were prepared by injection molding. The dumbbell-shape bars with dimensions of approximately 75 mm long ×2.5 mm thick and 4.0 mm wide at the narrowest section were produced using a WK-125 injection molding machine. The injection pressure was 60 MPa, the barred temperature was 210°C (all zones), and the nozzle temperature was 200°C.

Sample irradiation

The samples were irradiated in a UV-CURE device constructed in this laboratory.[10] The injection molded bars were irradiated by a medium pressure mercury lamp (Philips HPM 15), operated at 2 kW, at a distance of 10 cm from the surface of samples. The irradiation power measured on the surface of the samples, by means of a radiometer, was 4.0×10^{-2} W/cm^{-2}. The exposure was carried out in air at a temperature of about 60°C.

Measurements

Tensile properties

The tensile properties were measured using an Instron universal tester (Model 1185) at 25 ± 2°C with dumbbell-shape specimens at a crosshead speed of 25 mm/min, with an initial gauge length of 25 mm. Tensile strength (TS), tensile stress at break (TS_b), tensile stress at yield (TS_y), modulus of elasticity (E_t), and elongation at break (E_b) were recorded.

FTIR spectra

The FTIR spectra were recorded with a Nicolet MAGNA-IR 750 spectrometer. To minimize errors from sample thickness, the peak at 2720 cm^{-1} was used as an internal reference in this study. The relative absorbance intensity of C = O at 1723 cm^{-1} was expressed by the carbonyl index Abs. (1723 cm^{-1})/ Abs. (2720 cm^{-1}), where Abs. (1723 cm^{-1}) and Abs. (2720 cm^{-1}) were the absorbency at 1723 and 2720 cm^{-1}, respectively.

TABLE II
Tensile Properties and MFR of PP Samples Photodegraded for Different Times

Sample code	MFR[a] (g/10 min)	TS	TS_b	TS_y (MPa)	E_q	E_b (%)
H_1P_0	6.0	39.6	39.6	36.1	763	750
H_1P_{30}	7.5	37.3	37.3	35.6	686	630
H_1P_{60}	9.8	34.3	33.9	32.4	617	490
H_1P_{120}	13.6	30.4	30.4	29.3	525	240
H_1P_{180}	20.9	25.7	24.7	25.7	455	36
H_1P_{240}	28.7	20.1	19.0	20.1	367	22
H_2P_0	2.8	47.1	47.1	34.5	870	840
H_2P_{30}	3.4	45.6	44.9	34.4	709	790
H_2P_{60}	4.3	42.2	40.5	36.0	640	720
H_2P_{120}	5.9	40.8	40.7	35.6	523	630
H_1P_{180}	7.5	38.0	36.6	36.9	487	150
H_1P_{240}	8.5	31.9	30.4	31.3	445	110
CP_0	1.3	37.7	37.7	28.6	424	1100
CP_{30}	1.5	36.7	36.3	26.6	402	1020
CP_{60}	1.9	35.6	35.6	26.6	380	1000
CP_{120}	2.1	34.9	32.8	25.9	351	840
CP_{180}	2.4	30.7	30.7	25.1	329	510
CP_{240}	2.9	27.3	27.1	23.6	299	410

[a] The melt flow rate (MFR) was determined at 230°C under a load of 2.16 kg according to ASTMD-1238 stardard.

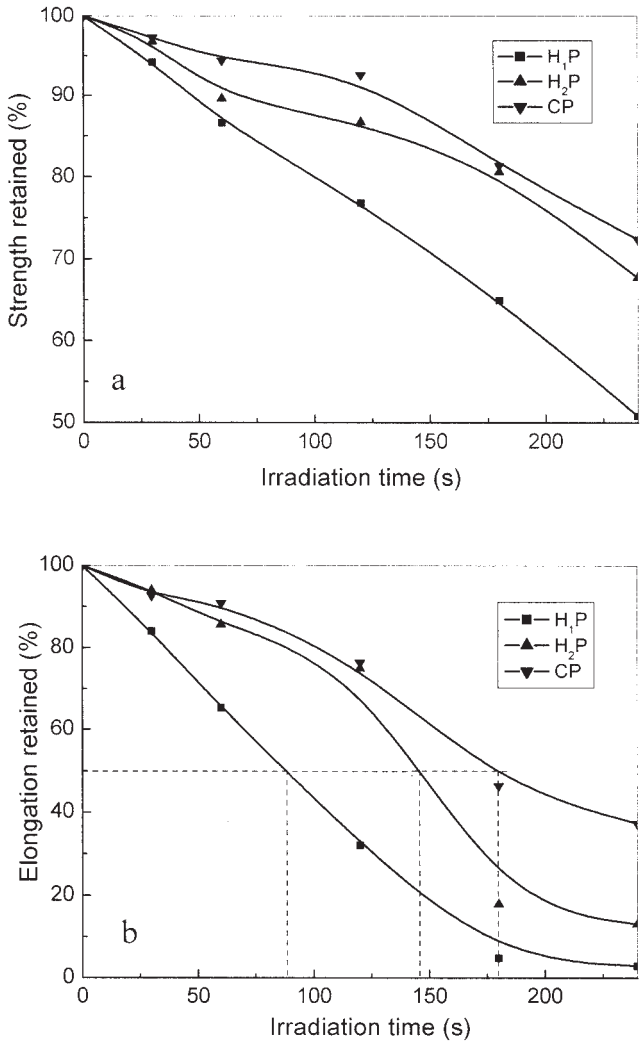

Figure 1 Evolution of mechanical properties of photodegraded PP samples versus irradiation time: (a) TS; (b) E_b.

XPS spectra

The XPS spectra were recorded with a VG ESCALAB MKII spectrometer, using Alkα excitation radiation ($h\nu$ = 1253.6 eV).

Surface morphological analysis

The surface morphologies of photodegraded PP samples were observed by a scanning electron microscope (SEM) (Hitachi X560 scanning electron microanalyzer, Japan). Before observation, the surface was coated with a conductive gold layer.

XRD

The wide angle X-ray diffractometer (WARD) pattern was recorded at room temperature with a D/max-rA rotating anode X-ray diffractometer (Riyaku Electrical Machine Co., Japan). The radiation from the Cu target was reflected from a graphite monochromator to obtain monochromatic CuKα radiation with a wavelength of 0.1541 nm. The generator was operated at 40 kV and 50 mA. The diffractograms were determined over a range of diffraction angle 2θ from 10 to 40° at a rate of 2°/min.

The apparent dimensions of a crystallite L_{hkl} along the direction perpendicular to the crystal plane hkl can be determined using the Scherrer equation,[11]

$$L_{hkl} = \frac{K\lambda}{\beta_0 \cos\theta}, \quad (1)$$

where L_{hkl} is the crystalline size along the direction perpendicular to reflecion plane (hkl) (nm), θ is the Bragg angle, λ is the wavelength of X-ray used (0.1541 nm), β_0 is the width of diffraction beam used (rad), K is the shape factor of a crystalline, being related to the shape of a crystalline and definition of β_0, when β_0 is defined as the half-height width of diffraction peaks, K = 0.9.

The relative content of β-form in PP were determined using the Turner–Jones equation[12] on the basis of a typical X-ray diffraction diagram,

$$k = \frac{H_{\beta 1}}{H_{\beta 1} + (H_{\alpha 1} + H_{\alpha 2} + H_{\alpha 3})}, \quad (2)$$

where k is the amount of the β-form, $H_{\beta 1}$ is the height of the strong single β-form (300), and H_α is the heights of the three equatorial α-form peaks (110), (040), (130).

Crystallization and melting behaviors

A Perkin–Elmer DSC-2 instrument was used to investigate the crystallization and melting behavior of pho-

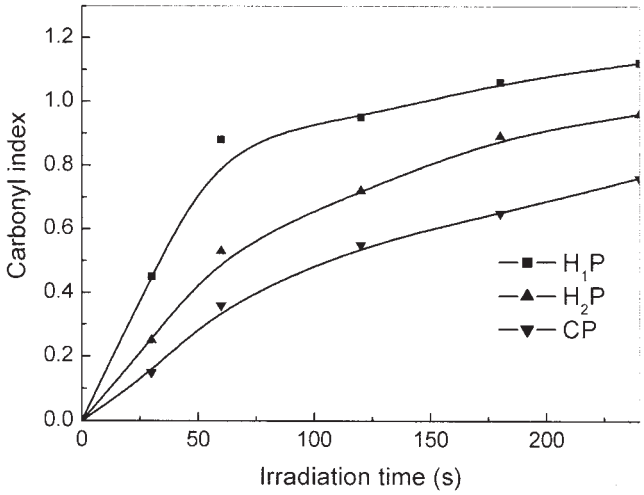

Figure 2 Changes of carbonyl indices in various photodegraded PP samples with irradiation times.

todegraded H_2P, programmed for a heat-fold-cool-heat cycle. The heating/cooling rate was 20°C/min and the temperature range was 60~200°C with a 5-min hold time. The crystallinity X_c was calculated by the relative ratio of the enthalpy of fusion per gram of samples to the heat of fusion of PP crystal (209 J/g).[13]

Dynamic mechanical properties

The dynamic mechanical properties of photodegraded H_2P were evaluated using a dynamic mechanical thermal analyzer-DMTA IV (Rheometric Scientific Co. Ltd.). The compression molded sample size was 30 $\times$ 8 $\times$ 1 mm^3. Testing was carried out in a temperature range of -50 to 50°C at a constant frequency of 5 Hz and a heating rate of 5°C/min. The temperature dependence on the loss tangent (tanδ) and storage modulus (E') was recorded.

RESULTS AND DISCUSSION

Mechanical properties

The UV-irradiation resistance of polymeric materials is best evaluated by measuring physical properties, such as elongation at break and tensile strength. The tensile properties of original and photodegraded PP samples are summerized in Table II. As can be seen from Table II, the melt flow rates (MFRs) of all photodegraded PP samples increase with increasing UV-irradiation times. For H_1P sample, the MFR increses more than fourfold when the UV-irradiation time up to 240 s, but for H_2P and CP, the MFRs increase about three times and twofold, respectively. MFR is a measurement of molecular weight. The extent of decrease in molecular weight, which is due to the chain scission by photodegradation, is the largest for H_1P, followed by H_2P, and then CP, indicating that CP possesses higher UV-irradiation stability than H_1P and H_2P. The mechanical properties, such as TS, E_t, and E_b, decrease with increasing UV-irradiation times, which is the main practial effect of chemical degradation in PP and results from the reduction in molecular weight. Figure 1 shows the evolution of mechanical properties of photodegraded PP sample as a function of UV-irradiation times. The elongation retained is the ratio of the elongation of irradiated sample against an unirradiated one. As shown in Figure 1a, the TS of H_2P and CP reduces gradually with increasing UV-irradiation time, whereas for H_1P, TS decreases significantly. The E_b (Fig. 1b) after irradiation shows the same characteristics as tensile strength as a function of irradiation times. The irradiation times taken to 50% reduction of elongation at break by degradation during irradiation extend from 88 s for H_1P and 145 s for H_2P to more

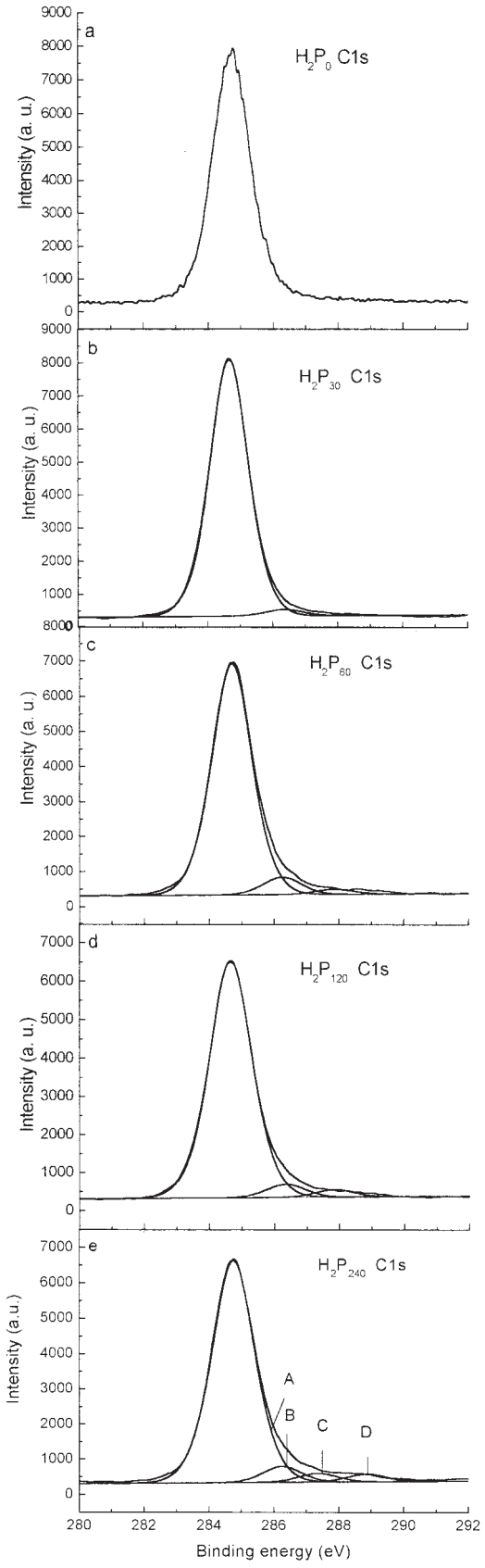

Figure 3 C1s XPS spectra of various PP samples photodegraded for different times.

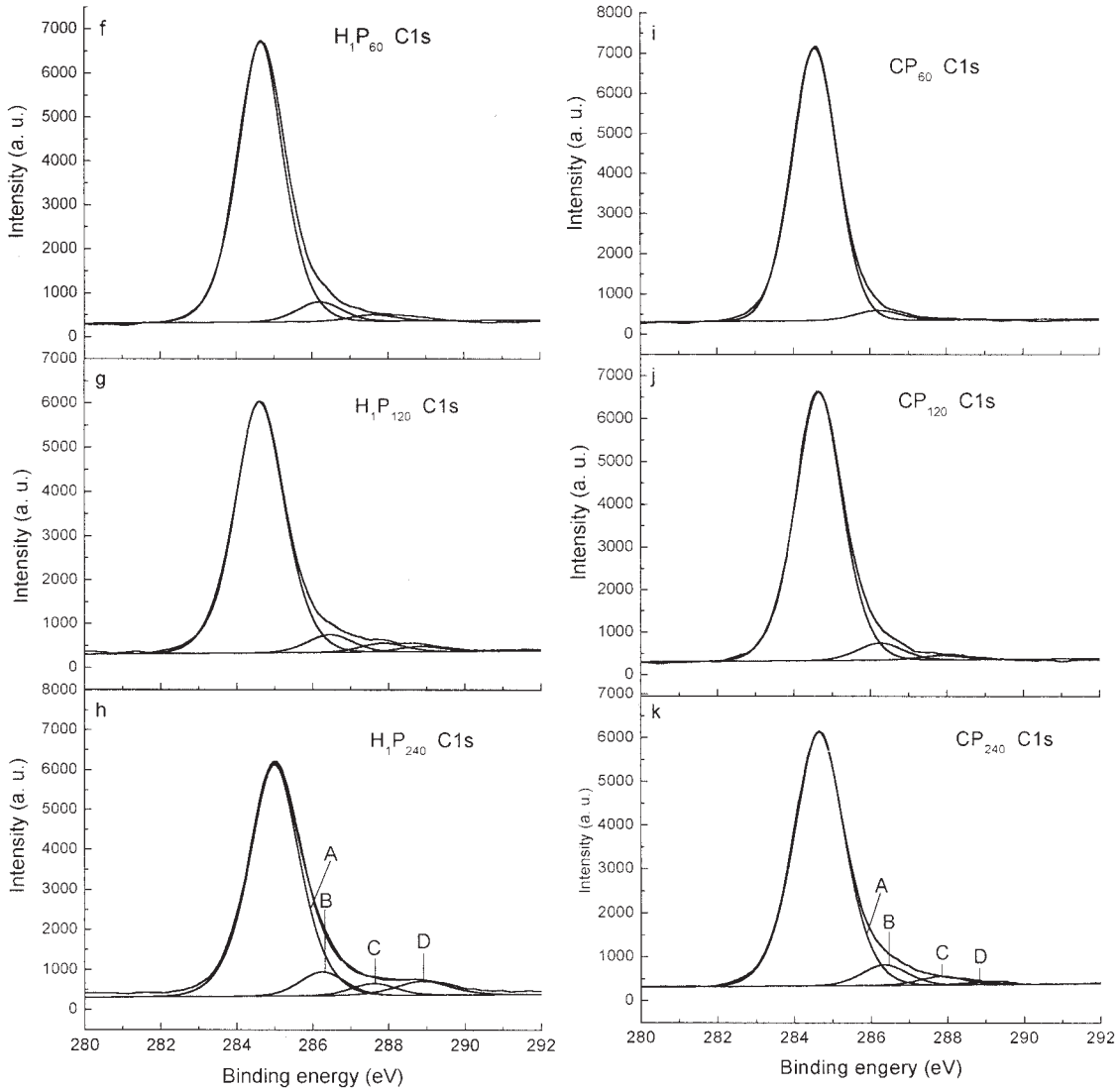

Figure 3 (*Continued from the previous page*)

than 180 s for CP. The results show that CP is of the highest UV-irradiation resistance.

Degree of oxidation

The carbonyl indices obtained from the FTIR spectra are used to characterize the degrees of oxidation of PP samples, as described in the experimental section. Figure 2 shows the changes in carbonyl indices of photodegraded PP samples with UV-irradiation times. The carbonyl index of each photodegraded PP sample increases apparently with increasing UV-irradiation times. However, the carbonyl index of H_1P is obviously higher than that of H_2P, whereas CP displays the least carbonyl index, manifesting that CP is the most stable against UV-irradiation, followed by H_2P and H_1P.

Surface photooxidation

It is well-known that XPS is effectively used to gather information in the outmost few tens of angstroms of the samples. In this paper, XPS was applied to study surface photooxidation of PP. Figure 3 shows the C1s XPS spectra of various PP samples photodegraded for different times. The decomposition of the C1s peak

TABLE III
O/C Atom Ratios of Various PP Irradiated for Different Times

O/C atom ratio	Unirradiated	30 s	60 s	120 s	240 s
F401	0	0.09	0.17	0.19	0.21
Co-PP	—	—	0.11	0.16	0.19
045–1	—	—	0.18	0.20	0.23

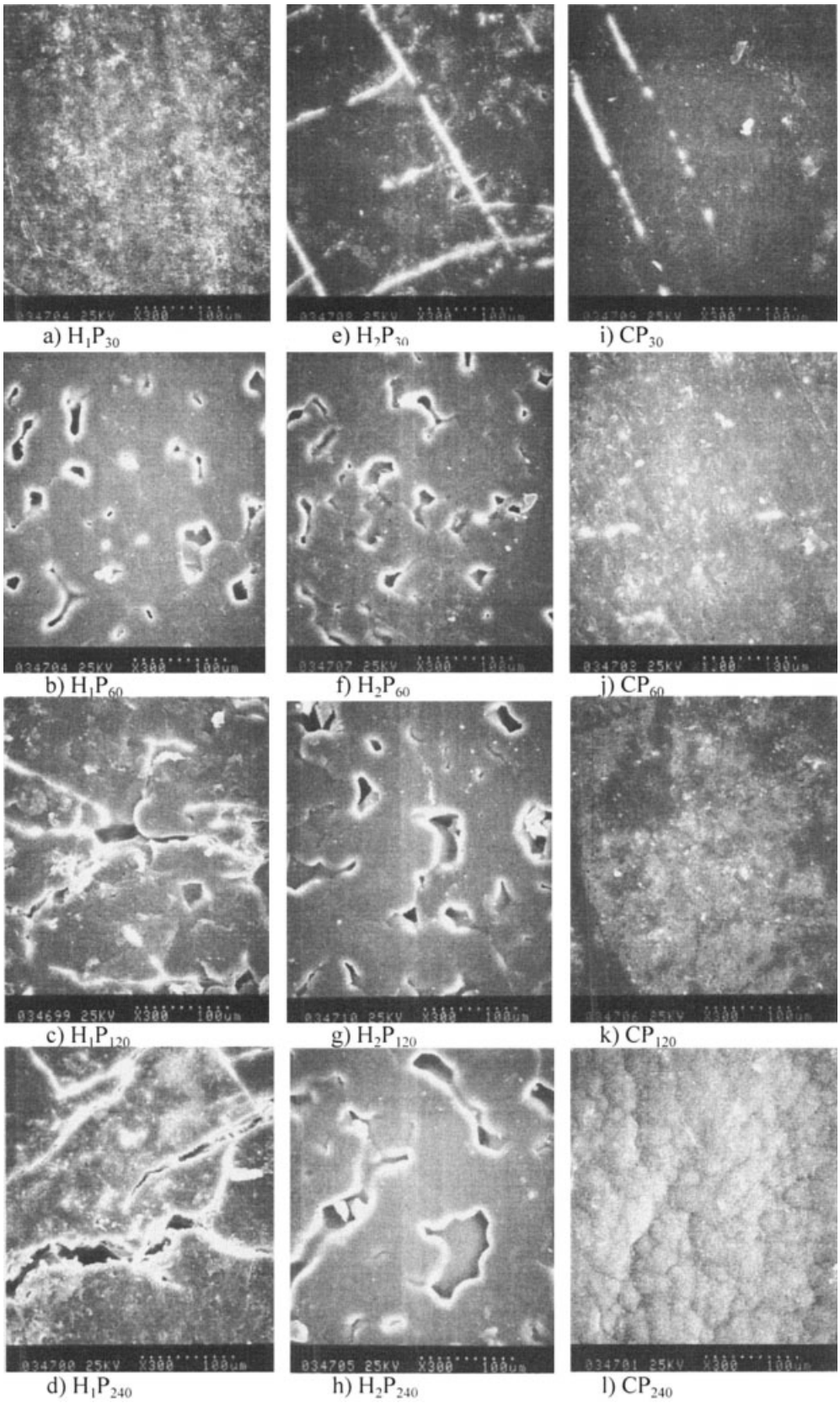

Figure 4 SEM micrographs of various PP samples photodegraded for different times.

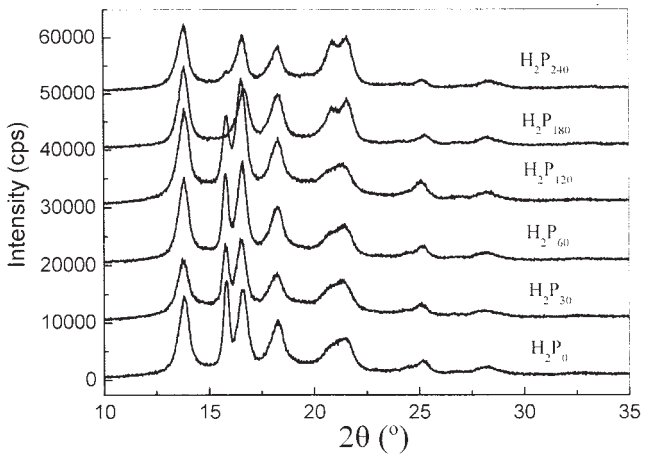

Figure 5 XRD diffractograms of H_2P photodegraded for different times.

was performed using literature data: CH_x at 285.0 eV; C-O at 286.5 eV; C = O at 288.0 eV, and ester or carboxyl at about 289.2 eV.[14] For all PP samples, the strong peak at 285.0 eV is due to the C1s electron from the C-C and C-H bonds of PP. The intensity of the small peak appears at 286~290 eV in the C1s band and increases with increasing UV-irradiation time, which indicates the formation of surface photooxidation products, such as -CH_2-O, -C(= O)-, and –C(= O)-O- groups. For H_2P and CP, only when UV-irradiated for up to 240 s, the fitter peak locating at 289.0 eV appears (Fig. 3e and k), which is attributed to iC(= O)-O- groups. However, for H_1P, when UV-irradiated for 120 s, the fitter peak at 289.0 eV emerges (Fig. 3g). Moreover, the area of the fitter peak at 286~290 eV of CP is smaller than that of H_2P and H_1P. For CP, even upon irradiation for 240 s, the fitter peak at 289.0 eV is very small, indicating that the extent of photooxidation of CP is the lowest, followed by H_2P and H_1P.

The stoichimetric O/C ratios obtained from the XPS spectra are used to characterize the degree of surface photooxidation. The O/C data of photodegraded PP samples are listed in Table III. It can be seen that the O/C atom ratios increase with increasing UV-irradiation times. CP possesses the lowest O/C atom ratio while H_1P dispalys the highest O/C atom ratio, which indicating that the degree of surface photooxidation of H_1P is the most severe, followed by H_2P and CP.

Morphology of photooxidized samples

SEM micrographs of various PP samples photodegraded for different times are shown in Figure 4. When H_1P was UV-irradiated for 30 s, there are numbers of pores on the surface (Fig. 4a), which is the consequence of chemicrystallization leading to contraction of the surface layer. However, for H_2P and CP, their surfaces seem ralative smooth (Fig. 4e and i). When H_1P was UV-irradiated for up to 240 s, big profound crackes appear (Fig. 4d); for H_2P, there are some big pores (Fig. 4h); but for CP, the photooxidized surface seem to be dense, there are no big pores or cracks allowing oxygen penetrating into the interior of sample (Fig. 4l). The appearance of microcracks would provide a higher oxygen pressure inside the strip, resulting in auto-oxidation.[15] Therefore, for H_1P, the big profound cracks lead to severe oxidation inside the strips, but for CP, the degree of oxidation was relative low, followed by H_2P.

TABLE IV
Crystalline Size and β-Form Crystal Content of Photodegraded H_2P

Sample code	L_{110}	L_{040} (nm)	L_{130}	β-Form crystal content (%)
H_2P_0	14.30	16.86	13.40	30.9
H_2P_{30}	14.55	17.61	13.44	29.3
H_2P_{60}	14.85	17.86	13.59	26.7
H_2P_{120}	15.45	17.63	13.87	22.1
H_2P_{180}	15.45	15.90	13.40	0
H_2P_{240}	14.28	15.50	13.29	0

Crystallization behavior

In Figure 5 the X-ray diffractograms of H_2P photodegraded for different times are compared. The important peaks characteristic of the α phase can be found at the scattering angles 2θ of 14.0° (110), 17.0° (040), 18.5° (130), 21.0° (111), and 22.0° (131 and 041), while the β phase can be detected by peak at 16° (300).[12] It can also be seen that, for unirradiated injection mouled H_2P

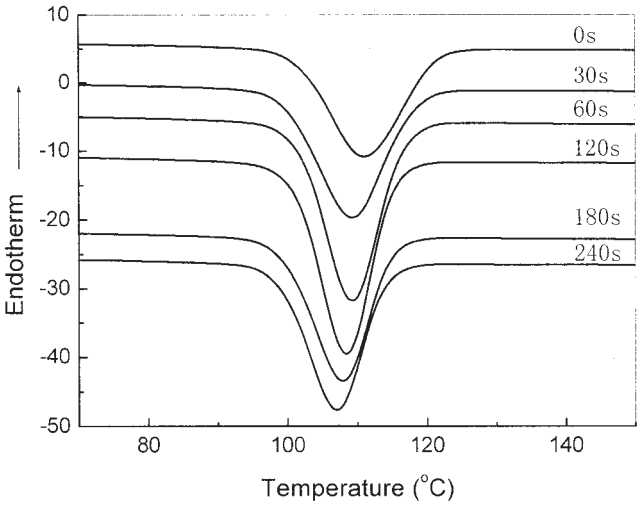

Figure 6 Crystallization behavior of H_2P sample photodegraded for different times.

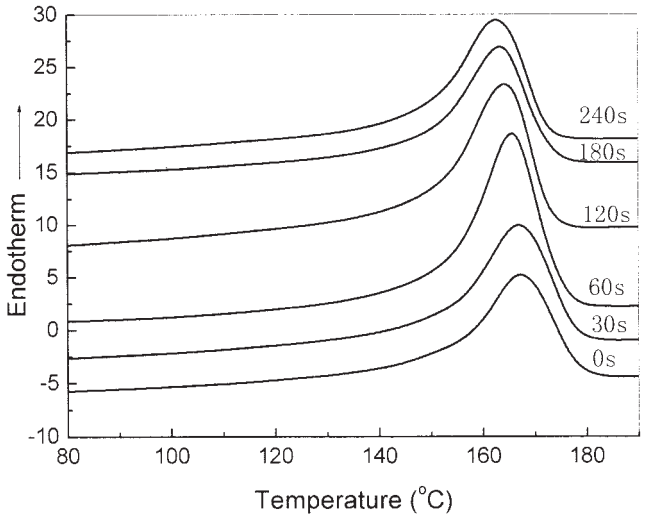

Figure 7 Melting behavior of H_2P sample photodegraded for different times.

sample, there are some β-form, which is usually found in PP specimens that have been subjected to mechanical deformation, e.g., in injection molded and extruded products.[16] The relative content of β-form and crystalline size are listed in Table IV. It can be seen from Figure 5 and Table IV that the β-form content decreases with increasing UV-irradiation time, and even disappeared entirely when irrdiated for up to 240 s, indicating that UV-irradiation induces the transformation of crystalline form, namely β-form changing into α-form. The transformation of the less stable β-form into the α-form upon heating or annealing has been since long known.[17,18] However, this phenomenon has been not yet reported in literature. Its possible explanation is that the molecular chains, which compose β-form, compact relatively loose compared with α-form and are prone to be photodegraded to shorter molecular chains, which rearrange into relative stable α-form. It is also interesting to note that the crystalline size increases with increasing UV-irradiation time, which is probably due to the shorter molecular chains of photodegraded samples possessing higher mobility, which gather into bigger crystallites. However, further prolonging irradiation time leads to a decrease of crystalline size, because a large number of chemical defects (e.g., carbonyl groups) in the chains prevent further crystallization. Moreover, the relative intensity of diffraction peaks differed with UV-irradiation time. When the irradiation time is beyond 60 s, the peak (040) is the strongest among the diffraction peaks characteristic of α-form, but when the iradiation time exceeded 60 s, peak (110) replaces the peak (040) as the strongest one. Moreover, peak (111) and the overlapping peak of (131) and (041) become stronger with increasing UV-irradiation times. The mechanism of the change of relative intensity for different peaks resulting from UV-irradiation is not clear, which, together with the transformation of crystalline form induced by UV-irradiation, is worthy of further investigation.

Thermal properties

The crystallization and melting behaviors of photodegraded H_2P are shown in Figures 6 and 7, respectively, and the corresponding thermal properties are presented in Table V. It can be seen from Figure 6 that the crystallization temperature, taken as the position of the maximum of exothermic peak, decreases with increasing UV-irradiation time, presumbly due to the progressively lower molecular weight and larger number of chemical irregularities present in the molecules of photodegraded PP. It is well known that shorter and defective molecules ctystallize more slowly,[19,20] and this is likely to be sure for the case of photodegraded PP, and consequently the photodegraded PP has to crystallize at relatively lower temperature. From Figure 7, it is evident that the melting range is shifted to lower temperture with increasing UV-irradiation times. The decrease in melting temperature of photodegraded H_2P is probably due to the reduction in molecular weight[9] and the increase in stereoirregularities.[21] It is interesting to note that the

TABLE V
Crystallization and Melting Behaviors of Photodegraded H_2P

Sample code	T_{conset}	T_c (°C)	T_{mc}	T_m	Heat of fusion (ΔH), J/g	Crystallinity (%)
H_2P_0	117.1	110.6	156.1	167.4	−65.3	31.2
H_2P_{30}	115.6	109.4	154.5	166.9	−74.0	35.4
H_2P_{60}	114.1	109.0	153.7	165.7	−76.5	36.6
H_2P_{120}	113.6	108.5	153.3	164.2	−65.4	31.3
H_2P_{180}	113.0	107.9	152.0	163.5	−62.7	30.0
H_2P_{240}	112.2	106.9	151.5	162.6	−61.2	29.3

T_{conset}, crystallization onset temperature; T_c, crystallization peak temperature; T_{mc}, melting onset temperature; T_m, melting peak temperature.

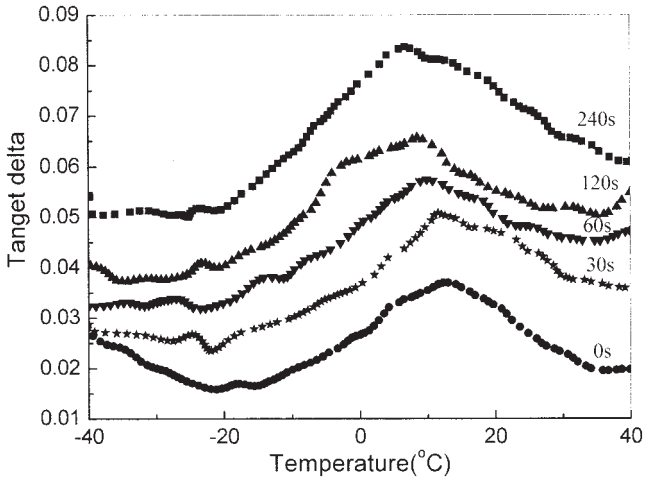

Figure 8 Loss tangent (tanδ) as a function of temperature at 5 Hz for H_2P samples photodegraded for different times.

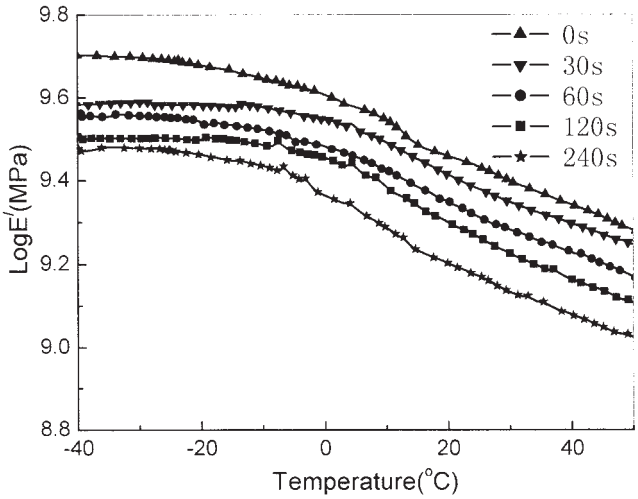

Figure 9 Storage modulus (E') as a function of temperature at 5 Hz for H_2P samples photodegraded for different times.

crystallinity of photodegraded H_2P increases with increasingUV-irradiation times up to 60 s, further prolonging irradiation time, the crystallinity begin to decrease. During the UV-irradiation, the scission of entangled molecules in the amphous phase is followed by the rearranglement of released segments, giving an increase in the melting enthalpy and consequent crystallinity. But when the UV-irradiation time exceeds over 60 s, the generation of impurity groups like carbonyls, limits the secondary crystallization by reducing the molecular regularity. At short-term exposures the chain scission effect dominates over irregularities and the crystallinity increases. When UV-irradiation time exceeds over 60 s, the large number of chemical defects in the chain prevent further crystallization, resulting in the decrease of crystallinity.[22]

Dynamic mechanical properties

The effect of photodegradation of H_2P on its dynamic mechanical properties are shown in Figures 8 and 9. The T_g's of original and photodegraded H_2P samples are listed in Table VI. From Figure 8, it is appearent that T_g, taken as the position of maximum of the loss tangent (tanδ) peak, decreases with increasing UV-irradiation time (see Table VI). The decrease of T_g amounts to 6°C when UV-irradiated for 240 s. According to Flory's free volume theory, the end groups have higher mobility than other parts in molecular chains. After photodegradation, the proportion of end groups increases, and consequently some chain units can move at relatively lower temperature, resulting in the decrease of T_g of PP. It can be seen from Figure 9 that the storage modulus decreases with increasing UV-irradiation time, which is due to the decrease of molecular weight resulting from photodegradation. Therefore, photodegradation results in the loss of rigidity of PP, which correlates well with the mechanical properties described in the former section.

The reason for CP, although possessing lower crystallinity and isotacticity, having better UV-irradiation stability than H_2P and H_1P is possibly due to that, in comparison with ethylene units, propylene units are by far the most photooxidizable [1, b]. Therefore, a certain amount of ethylene units in the chains can improve the photostability of PP. In comparison with H_2P, H_1P possesses the equivalent crystallinity and isotacticity, only differs in synthesis methods. However, the photostability of H_1P is worse than that of H_2P. For H_1P, its molecular weight distribution is wider, and consequently the proportion of molecules with lower molecular weight is relatively larger, which results in poorer radiation stability.[23]

CONCLUSION

The results from the measurements of MFR, mechanical properties, FTIR spectra, SEM, and XPS spectra have shown that CP has the highest UV-irradiation stability, followed by H_2P, and then H_1P, due to containing ethylene units. The synthesis method of PP palys an important role in the resistance to UV-irradiation. UV-irradiation induces the transformation of β-form to α-form of PP and the change in relative intensity of diffraction peaks.

TABLE VI
T_g of H_2P Photodegraded for Different Times

Irradiation time (s)	0	30	60	120	240
T_g (°C)	12.8	11.5	9.8	8.3	6.7

References

1. Delprat, P.; Duteurtre, X.; Gardette, J. L. Polym Degrad Stab 1995, 50, 1.
2. Yoshii, F.; Sudratat, A.; Binh, D.; Makuuchi, K.; Nishimoto, S-I. Polym Degrad Stab 1998, 60, 393.
3. Meligi G, Yoshii F, Sasaki T, Makuuchi K, Rabie AM, Nishimoto S-I. Polym Degra Stab 1997, 57, 241.
4. Rabello, M. S.; White, J. R. Polym Degrad Stab 1997, 56, 55.
5. Rabello, M. S.; White, J. R. J Appl Polym Sci 1997, 64, 2505.
6. Zhang, Z. F.; Hu, X. Z.; Luo, Z. B. Polym Degrad Stab 1996, 51, 93.
7. Qiao, J. L.; Wei, G. S.; Zhang, J. H.; Zhang, F. R.; Hong, X.; Wu, J. L. Radiat Phys Chem 1996, 48, 771.
8. Wei, G. S.; Qiao, J. L.;Hong, X.; Zhang, F. R.; Wu, J. L. Radiat Phys Chem 1998, 52, 237.
9. Yoshii, F.; Makuuchi, K.; Ishigaki, I. Die Angew Makromol Chem 1986, 143, 77.
10. Qu, B. J.; Rånby, B. J Appl Polym Sci 1993, 48, 701.
11. Alesander, L. E. X-Ray Diffraction Methods in Polymer Science; Wiley Interscience, New York, 1969.
12. Turner-Jones, A.; Aizlewood, J. M.; Beckett, D. R. Makromol Chem 1964, 75, 134.
13. Silva, A. L. N.; Coutinho, F. M. B.; Rocha, M. C. G.; Travares, M. I. B. J Appl Polym Sci 1997, 66, 2005.
14. Beamson, G., Briggs, D. High Resolution XPS of Organic polymers. The Scienta ESCA 300 Database, Wiley Chichester 1992.
15. Boss, C. R.; Chien, J. C. W. J Polym Sci Part A 1966, 4, 699.
16. Vleeshouwers, S. Polym 1997, 38(13), 3213.
17. Padden, F. J.; Keith, H. D. J Appl Phys 1959, 30, 1479.
18. Nata, G.; Corradini, P. Nuovo Cimento 1960, 15, 40.
19. Martuscelli, E.; Prucella, M.; Crispino, L. Polym 1986, 24, 693.
20. Janimak, J. J.; Cheng, S. Z. D.; Giusti, P. A.; Hsieh, E. T. Macromolecules 1991, 24, 2253.
21. Cheng, S. Z. D.; Janimak, J. J.; Zhang, A.; Hsieh, E. T. Polymer 1991, 32, 648.
22. Rabello, M. S.; White, J. R. Polymer 1997, 38, 6383.
23. Yoshii, F.; Makuuchi, K.; Ishigaki, I. Polymer 1988, 29, 146.